

Authors response on minor comments frpm Referee #2

Text in blue is original comment from referee followed by a reply and the actions done to improve the manuscript. A track-changes version of manuscript is find at the end of the pdf.

(1) Although this is not a comment for the manuscript, we cannot see a reference cited in response to minor comments 2 of referee #2.

Reply: This was a field code linking to a Figure. In parenthesis it was written: "(see Figure S3)" but after moving Figures there was an error message. Thus, it is not a reference. In the manuscripth there was no error.

(2) Lines 84-85. The authors wrote, "while favouring ON formation (reaction 1)", but it may still lead readers' misunderstanding. Can you suggest here that the yield of reaction 1 is 0.3 at most?

Action: Bold text was added to the sentence: " "while favouring **some** ON formation (reaction 1 **with a yield of up to 0.3**)"

(3) Line 175. The m/z of C5H6O12 should be 258.

Action: Done.

(4) Lines 210-216. The authors irradiated 254 nm light, which might induce the photolysis of aldehydes and peroxides, to the full length of the flow reactor; this is also a difference from Molteni et al.

Reply: We do not agree on adding a speculation on photolysis of aldehydes/peroxides. The estimated photon flux (1.6×10^{16} photons $\text{cm}^{-2} \text{s}^{-1}$) combined with typical aldehyde/peroxide cross sections of $10^{-20} \text{ cm}^2 \text{ molecule}^{-1}$ will give lifetimes of several thousands of seconds (the residence time is 30s). However, we can add a statement on that the OH was produced by irradiation at 254 nm.

Action: "In addition we produce OH radicals **through irradiation at 254 nm** in the full length of the flow reactor enhancing the effects of secondary chemistry." (bold text was added)

(5) Line 278. The word, "increases", might be "increased".

Action: Done.

(6) Line 334. The expression, "the yield of ON from NO+RO2 might be high", is again vague. Can you suggest here that the yield of reaction 1 is 0.3 at most?

Action: "the yield of ON from NO+RO2 might be **significant (e.g. up to 0.3)**" (bold text was changes)

(7) Line 373. Please revise equation 13. The reactant, "C9H14NO8-12x", should be "C9H14NO9-13". The term, "+ O2", should be added to the left hand side.

Action: Done

(8) Line 411. The words, ", right panels", could be removed.

Action: Done

(9) Lines 440-443. From present results, can the authors suggest a region of NO level, in which the found transition occurs in urban air?

Reply: Unfortunately, this cannot be directly derived from our experiments. The region would be when the NO reaction is competing with autoxidation and for sure that will be at rather low NOX but to really pin-point this one need to do a kinetic study.

Action: No action

1 **Effect of NO_x on 1,3,5-trimethylbenzene (TMB) oxidation product distribution and particle**
2 **formation**

3
4 Epameinondas Tsiligiannis¹, Julia Hammes¹, Christian Mark Salvador¹, Thomas F. Mentel^{1,2}, Mattias
5 Hallquist^{1*}

6 ¹Department of Chemistry and Molecular Biology, University of Gothenburg, Gothenburg, Sweden

7 ²Institute of Energy and Climate Research, IEK-8: Troposphere, Forschungszentrum Jülich GmbH,
8 Jülich, Germany

9 * *Correspondence to:* hallq@chem.gu.se

10 **Abstract**

11 Secondary organic aerosol (SOA) represents a significant fraction of the tropospheric aerosol
12 and its precursors are volatile organic compounds (VOC). Anthropogenic VOCs (AVOC) dominate
13 the VOC budget in many urban areas with 1,3,5-trimethylbenzene (TMB) being among the most
14 reactive aromatic AVOCs. TMB formed highly oxygenated organic molecules (HOM) in NO_x free
15 environment, which could contribute to new particle formation (NPF) depending on oxidation
16 conditions were elevated OH oxidation enhanced particle formation. The experiments were performed
17 in an oxidation flow reactor, the Go:PAM unit, under controlled OH oxidation conditions. By addition
18 of NO_x to the system we investigated the effect of NO_x on particle formation and on the product
19 distribution. We show that the formation of HOM and especially HOM accretion products, strongly
20 varies with NO_x conditions. We observe a suppression of HOM and particle formation with increasing
21 NO_x/ΔTMB and an increase in the formation of organonitrates (ON) mostly at the expense of HOM
22 accretion products. We propose reaction mechanisms/pathways that explain the formation and
23 observed product distributions with respect to oxidation conditions. We hypothesize that, based on our
24 findings from TMB oxidation studies, aromatic AVOCs may not contribute significantly to NPF under
25 typical NO_x/AVOC conditions found in urban atmospheres.

26 **1 Introduction**

27 Volatile organic compounds (VOC) are ubiquitous in the atmosphere and major precursors for
28 secondary organic aerosol (SOA). SOA represents a dominant fraction of the tropospheric aerosol
29 (Hallquist et al., 2009; Shrivastava et al., 2017; Gentner et al., 2017) and affects climate
30 (Intergovernmental Panel on Climate, 2014) and health (WHO, 2016). Consequently research interest
31 in SOA formation and properties is ranging from remote atmospheres (Ehn et al., 2012; Ehn et al.,
32 2014; Kristensen et al., 2016) to densely populated and polluted environments (Chan and Yao,
33 2008; Hu et al., 2015; Guo et al., 2014; Hallquist et al., 2016). Following the study by Ehn et al. (Ehn
34 et al., 2012), highly oxygenated organic molecules (HOM) with low volatilities, formed from the
35 oxidation of biogenic volatile organic compounds (BVOCs), have attracted much research interest
36 (Crouse et al., 2013; Ehn et al., 2014; Jokinen et al., 2014; Jokinen et al., 2015; Mentel et al., 2015; Yan
37 et al., 2016; Berndt et al., 2016; Bianchi et al., 2019). These compounds have been shown to contribute
38 to new particle formation (NPF) and to SOA growth (Ehn et al., 2014; Bianchi et al., 2016; Kirkby et
39 al., 2016; Trostl et al., 2016; McFiggans et al., 2019), making them an important factor in the formation
40 of atmospheric SOA. These oxidation products can be either described as HOM based on their high
41 oxygen number ($O > 6$) (Bianchi et al., 2019) or as extremely low volatile organic compounds
42 (ELVOC) based on their volatility (Donahue et al., 2012; Trostl et al., 2016). In this study, we will
43 refer to oxidation products as HOM, because not all of the measured compounds may fulfill the

44 criteria for ELVOC (Trostl et al., 2016; Kurtén et al., 2016). Gas phase autoxidation of alkylperoxy
45 radicals (RO₂) has been proposed as the formation mechanism for HOM (Crouse et al., 2013; Ehn et
46 al., 2014; Jokinen et al., 2014). After the initial reaction of an oxidant with the VOC and subsequent
47 addition of O₂ to the alkylradical (R), the produced RO₂ isomerizes via intra molecular H abstraction
48 (H-shift). During this process a hydroperoxide group and a new R is formed. Additional O₂ addition
49 and H-shift sequences can introduce large amounts of oxygen to the molecule and subsequently lower
50 the vapour pressure. The chemistry of aromatic compounds is somewhat different compared to other
51 VOCs as they can lose their aromaticity during the initial OH attack while they can retain the ring
52 structure. Moreover, reaction products are more reactive than the parent compound. The produced RO₂
53 form an oxygen bridge, a bicyclic and potentially a tricyclic alkylradical (Molteni et al., 2018; Wang et
54 al., 2017) before further oxidation processes open the ring structure. For 1,3,5-trimethylbenzene
55 (TMB), emitted from combustion sources in the urban environment, Molteni et al. (2018) proposed a
56 generalized reaction scheme for HOM formation after OH addition. According to their scheme, first
57 generation alkylperoxy radicals with the general formula of C₉H₁₃O₅₋₁₁ were formed from the initial
58 OH attack and subsequent H shift and O₂ addition sequences. A postulated second OH attack would
59 result in propagating peroxy radical chains yielding radicals with the general formulas C₉H₁₅O₇₋₁₁.

60 Generally, the termination reaction of RO₂ (with a general $m/z = x$) with HO₂, leads to the
61 formation of hydro peroxides ($m/z = x + 1$) while termination reactions with other RO₂ can lead to the
62 formation of a carbonyl ($m/z = x - 17$), a hydroxy group ($m/z = x - 15$) or dimers ($m/z = 2x - 32$)
63 (Mentel et al., 2015; Jokinen et al., 2014; Rissanen et al., 2014). The propagation reaction of RO₂ with
64 another RO₂ or NO also results in the formation of RO ($m/z = x - 16$). The RO can undergo internal H
65 shift leading to the formation of a hydroxy group and subsequent a new peroxy radical which can
66 continue the autoxidation sequences. The alkoxy step shifts of the observed m/z by 16 leads to overlap
67 of different termination product sequences. During extensive oxidation the first generation products
68 are subject to secondary chemistry increasing the numbers of products. Molteni et al. (Molteni et al.,
69 2018) found several closed shell monomer products with the general formula C₉H₁₂₋₁₆O₅₋₁₁ from the
70 oxidation of TMB with OH. The formation of dimers with different number of H atoms in their study
71 was explained by reactions of two first generation RO₂ radicals (C₁₈H₂₆O₅₋₁₀), one first and one second
72 generation RO₂ (C₁₈H₂₈O₉₋₁₂) or two second generation RO₂ resulting in the dimer C₁₈H₃₀O₁₁. Although
73 dimers have in general lower O:C ratios than monomers, they are expected to be less volatile due to
74 higher molecular weight and more functional groups making them candidates to participate in
75 nucleation processes (Kirkby et al., 2016).

76 Organonitrates (ON) are formed as soon as sufficient NO_x is present in the atmosphere. ON
77 are highly important for the reactive nitrogen budget wherein the formation of highly functionalized
78 organic nitrates can contribute significantly to secondary organic aerosol (Lee et al., 2016; Bianchi et
79 al., 2017). In this study we refer to compounds that only consist of H, C and O as HOM monomers or
80 HOM dimers and to N containing compounds as ONs.

81 NO_x influences the oxidation of organics directly by changing oxidant levels (reducing or
82 increasing OH, depending on the NO_x regime) and indirectly by influencing RO₂ chemistry. In high
83 NO_x environment such as urban areas the reaction of NO with RO₂ radicals can compete with the
84 autoxidation mechanism (reaction 1 and 2) and thus potentially inhibit HOM while favouring [some](#)
85 ON formation (reaction 1 [with a yield of up to 0.3](#)).



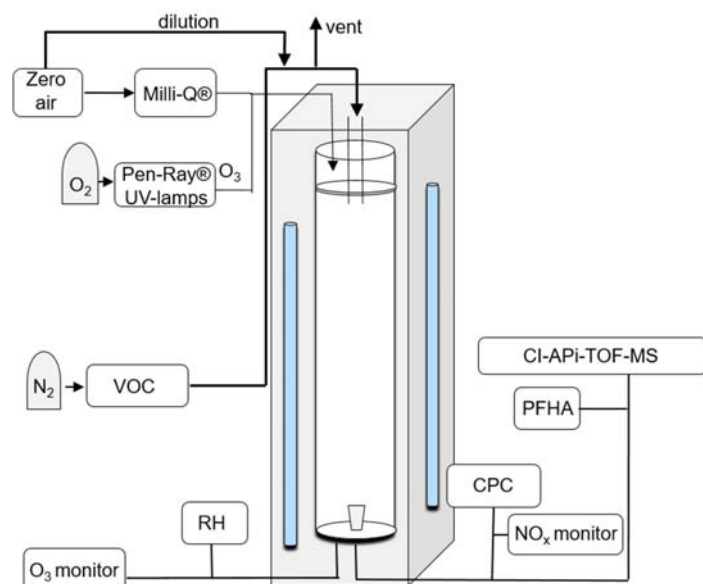
88 Although ON may have high O:C they differ from HOM as they contain at least one nitrogen atom.
89 While HOM formation from BVOCs has been intensively studied, only few studies have been
90 conducted focusing on the formation of HOM from anthropogenic aromatic volatile organic

91 compounds (AVOCs) (Molteni et al., 2018; Wang et al., 2017). However, these studies indicate that
92 AVOCs have a strong potential to form HOM under NO_x free conditions and proposed that they may
93 play a crucial role in NPF and particle growth of SOA in urban areas. Regarding SOA yields a number
94 of smog chamber studies have been conducted in order to investigate the oxidation of TMB with OH
95 radical under different NO_x and aerosol seed conditions (Paulsen et al., 2005; Rodigast et al.,
96 2017; Wyche et al., 2009; Huang et al., 2015; Sato et al., 2012). They reported that under higher
97 NO_x:VOC conditions, SOA yield is reduced compared to medium or lower NO_x:VOC conditions. The
98 NO_x:VOC, in almost all studies, was < 1, apart from one experiment (Wyche et al., 2009), with
99 NO_x:VOC = 1.9 in which the SOA yield was 0.29, compared to yields up to 7.47 under lower NO_x
100 conditions.

101 In this study we investigate the oxidation of TMB in a laminar flow reactor, while different
102 NO_x and OH conditions were applied. A nitrate chemical ionization atmospheric pressure interface
103 time of flight mass spectrometer (CI-API-TOF-MS) (Junninen et al., 2010; Jokinen et al., 2012) was
104 used to monitor the oxidation product distribution. We show the formation of HOM and nitrate
105 containing compounds with and without NO_x added to the reaction system. Possible mechanisms
106 leading to the formation of ON and suppression of particle formation are discussed.

107 2 Materials and Methods

108 The measured HOM were generated using the laminar flow Gothenburg Potential Aerosol
109 Mass reactor (Go:PAM), initially described by Watne et al. (Watne et al., 2018). The Go:PAM is a
110 100 cm long, 9.6 cm wide quartz glass cylinder which is irradiated over a length of 84 cm by two 30
111 W Phillips TUV lamps (254 nm); a schematic is shown in Figure 1. The OH radicals are produced
112 inside Go:PAM by photolyzing O₃ in the presence of water vapour. The O₃ is generated outside
113 Go:PAM by photolyzing pure O₂ (UVP Pen-Ray® Mercury Lamps, 185 nm) and distributed in 3 L
114 min⁻¹ particle free and humidified air (Milli – Q) over the reactor cross section. The VOC was
115 introduced through a gravimetrically characterized diffusion source (see Figure S2) centrally at the top
116 of the reactor with a flow of 8 L min⁻¹ while NO was introduced via a NO gas cylinder. Flows were
117 adjusted for a median residence time of 34 s in Go:PAM. A funnel shaped device is subsampling the
118 centre part of the laminar flow to minimize wall effects on the sample. A condensation particle counter
119 (CPC, 3775 TSI) was used to measure the number particle concentration in the sample flow. O₃ was
120 monitored by a model 202 monitor (2B Technologies), relative humidity by a Vaisala HMP60 probe
121 and NO_x by a model 42i monitor (Thermo Scientific) over the course of the experiments. The OH
122 exposure, over the residence time in the reactor, for NO_x free conditions without added TMB was
123 measured using SO₂ titration (Teledyne T100) as described by Kang et al. (Kang et al., 2007). Gas
124 phase oxidation products were measured with an Atmospheric Pressure interface High Resolution
125 Time of Flight Mass Spectrometer (API-TOF-MS, Aerodyne Research Inc. & ToFwerk AG) (Junninen
126 et al., 2010; Jokinen et al., 2012) in connection with a A70 CI-inlet (Airmodus Ltd) (Eisele and Tanner,
127 1993). The CI inlet is a laminar flow inlet operated with a sheath flow of 20 L min⁻¹ containing NO₃⁻
128 ions which are generated by ionizing HNO₃ using an ²⁴¹Am foil upstream in the inlet design. The
129 sample stream from Go:PAM is introduced in the centre of the sheath flow at a rate of 8 L min⁻¹. The
130 NO₃⁻ ions are electrostatically pushed into the sample flow and form stable adducts with sample
131 molecules as described by Ehn et al. (2012). The reaction time of oxidation products and NO₃⁻ is a few
132 hundred ms before being subsampled into the TOF-MS at 0.8 L min⁻¹ by a critical orifice. Differential
133 pumping decreased the pressure from 103 mbar in the CI source to 10⁻⁶ mbar in the TOF extraction
134 region where HOM are detected as negatively charged clusters with NO₃⁻.



135
 136 **Figure 1: Schematics of the experimental setup with Go:PAM chamber connected to CI- API-**
 137 **TOF-MS.**

138 A kinetic box model was used to simulate the chemistry in the Go:PAM reactor. The core of
 139 the model were first described by Watne et al. (Watne et al., 2018). The model consists of 32 species
 140 and 68 reactions now including TMB chemistry partly from the MCM v3.3.1 (Jenkin et al., 2003) as
 141 well as proposed mechanisms and rate coefficients for NO₂ chemistry (Atkinson et al.,
 142 1992; Finlayson-Pitts, 1999) and highly oxygenated compounds (Ehn et al., 2014; Berndt et al., 2018;
 143 Zhao et al., 2018) (see SI Table S2). The photon flux used in the simulations was tuned to match
 144 measured decay of O₃ while an OH sink was added to match the observed OH exposure in the
 145 background experiment, i.e. without the addition of TMB. The model was run for all experiments with
 146 and without NO_x. Primarily, the modelled output on OH exposure for each experiments was used to
 147 interpret the results and for calculating the consumed TMB. However, broadly the modelling output
 148 was also used to understand the effects of changing experimental conditions on monomer, dimer and
 149 organonitrate (ON) production. The experiments without NO_x were named 1-4 denoting the increase
 150 in OH exposure and experiments with NO_x were denoted according to their NO_x/ ΔTMB and high (H)
 151 and low (L) OH exposure as seen in Table 1.

152 3 Results and Discussions

153 Table 1 summarises eight experiments where TMB has been oxidised by various amounts of
 154 OH using the Go:PAM unit. Generally, a high OH production, induced either by increased light
 155 exposure (two lamps) or elevated ozone concentration, resulted in new particles (e.g. exp 3 and 4)
 156 while addition of NO_x reduced or suppressed the particle formation. The results from the kinetic model
 157 show that the amount of reacted TMB ranges from 5 – 30 ppb, depending on OH exposure (SI Figure
 158 S1). An overview of the oxidation product distribution measured with the CI- API-TOF-MS for

159 different conditions is shown in Figure 3 and 4. The compounds were detected as nitrate clusters at m/z
 160 = $mass_{\text{compound}} + 62$. The spectra in Figure 3 and 4 show significant ion signals from oxygenated
 161 hydrocarbons retaining the 9 carbons from the original TMB with either even H numbers (closed
 162 shell) or odd H numbers (open shell) with limited amount of products from fragmentation, i.e. ions
 163 with less than nine C. C_9 compounds with an O/C ratio of 6/9 or higher were classified as HOM
 164 monomers with the general formula $C_9H_{12-16}O_{6-11}$ in the mass range 280 – 360 m/z . Oxygenated
 165 hydrocarbons found in the range 460 – 560 m/z containing 18 C were classified as dimers with
 166 chemical formulas $C_{18}H_{24-30}O_{10-16}$. The monomer with the highest intensity detected was $C_9H_{14}O_7$ m/z
 167 296. The highest intensities among the dimers were $C_{18}H_{26}O_{10}$, $C_{18}H_{28}O_{11}$ and $C_{18}H_{28}O_{12}$ at m/z 464,
 168 m/z 482 and m/z 498, respectively. In addition to HOM monomers and dimers, nitrogen containing
 169 compounds were found as C_9 compounds with one or two N or C_{18} compounds with one N. The
 170 nitrogen containing compounds were of the general formulas $C_9H_{12-18}NO_{6-13}$, $C_9H_{12-18}N_2O_{8-15}$ and
 171 $C_{18}H_{18-24}NO_{6-10}$. The dominating ON were $C_9H_{13}NO_8$ at m/z 325, $C_9H_{15}NO_{10}$ at m/z 359 and
 172 $C_9H_{14}N_2O_{10}$ at m/z 372 respectively. In the experiments where NO_x was added, the formation of ON
 173 compounds was increasing with the NO_x concentration. In parallel, the levels of HOM monomers and
 174 dimers were reduced with NO_x concentration, where dimers were stronger affected than monomers.
 175 Even if the fragmentation products were limited some fragmentation leading to less than 9 carbons
 176 could be observed. The most prominent fragments were assigned molecular formulas $C_4H_7NO_7$ at m/z
 177 243, $C_4H_6O_{12}$ at m/z 246, $C_5H_6O_{12}$ at m/z 285-258 and $C_6H_9NO_7$ at m/z 269. Some compounds with C
 178 numbers of 15 and 17 were detected in the range 270 – 560 m/z but their contribution to the total
 179 signal was negligible (Figure 3).

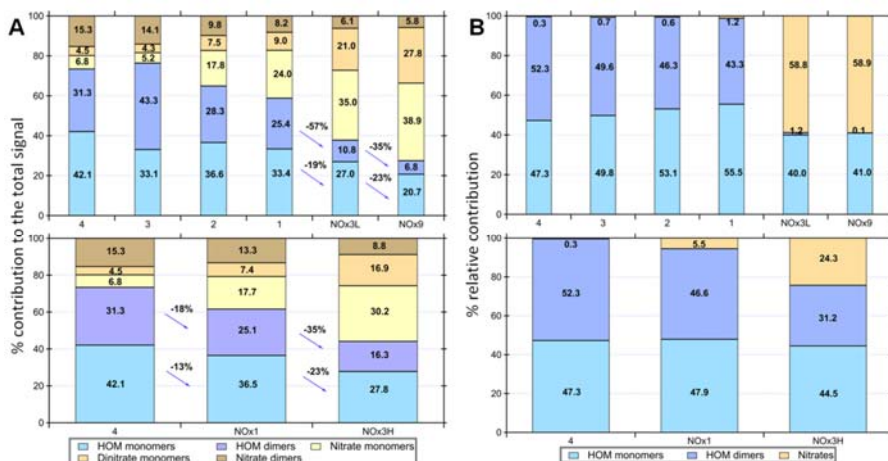
180

181 **Table 1: Experimental conditions for experiments with 30 ppb TMB. Ozone and initial NO_x**
 182 **concentration at time 0 are given in ppb and explicitly modelled OH exposure in molecules $s\ cm^{-3}$**
 183 **3 . TMB reacted (Δ TMB) in ppb after a reaction time of 34 s and particle number concentration**
 184 **given in $\#\ cm^{-3}$ after reaching steady state in Go:PAM. RH in all experiments was 38%.**

#	$[O_3]_0$	$[NO_x]_0$	OH exposure	Δ TMB	NO_x / Δ TMB	Particle number	Contribution of top 10 species (%)
1	~19	5	3.5×10^9	5.4	0.9	-	28.6
2	~19	5	7.1×10^9	9.9	0.5	-	29.8
3	~100	3	3.8×10^{10}	26	0.1	60 ± 14	38.6
4	~100	3	2.1×10^{11}	30	0.1	1610 ± 217	35.9
NO_x9	~9	82	6.3×10^9	9	9.1	-	52.4
NO_x3_L	~12	38	7.9×10^9	11	3.5	-	42.3
NO_x3_H	~100	79	3.1×10^{10}	25	3.2	-	34.2
NO_x1	~100	35	9.1×10^{10}	30	1.2	170 ± 50	30.5

185

186 The relative contribution of the different compound classes to the total assigned signal are shown in
 187 Figure 2. It is apparent that HOM monomers and dimers dominate in the experiments with low NO_x .
 188 The contribution of the monomers to the total oxidation product signal ranges from 20.7- 42.1% and
 189 dimers make 6.8 – 43.3 % of the total, depending on experimental conditions. Dimer contributions are
 190 highest at high OH exposure (exp 3 and 4 with estimated OH exposure of 3.8×10^{10} and 2.1×10^{11}
 191 molecules $s\ cm^{-3}$, respectively) and decrease with increasing NO_x . Nitrated compounds dominated the
 192 spectra with contributions up to ~75% in the experiments with highest amount of NO_x . Surprisingly,
 193 some nitrated compounds were also found in the experiments without added NO_x which may stem
 194 from background NO contamination (~3-5ppb).



195
196 **Figure 2: A) Overview of different compound groups to the total explained signal. Top panel**
197 **illustrates the influence of a decrease of OH exposure (exp 4 - exp 1) and further decrease after**
198 **adding NO_x in exp NO_x3L – exp NO_x9. Dimers show a larger relative reduction than monomers**
199 **with increasing NO_x/VOC. Bottom panel shows the influence of increased NO_x/VOC on the**
200 **product distribution. Experiments 4, 3 and NO_x1 resulted in particle formation. B) Modelled**
201 **product distribution shown as lumped categories of nitrated compounds, HOM monomers and**
202 **dimers and their relative contributions**

203 Recently, Molteni et al. (2018) assigned 17 compounds making up 80% of the total detected signal for
204 HOM oxidation products from the reaction of TMB with OH. Their compound with the highest
205 fraction of the signal (24.2%) was the dimer C₁₈H₂₆O₈. This compound was not detected in our study.
206 We did neither detected deprotonated compounds in the mass range 270 – 560 *m/z* nor HOM
207 monomers with 17 H nor compounds with O/C<0.55 which were found by Molteni et al. (2018).
208 However, we do find 10 of the previously reported 17 monomers and dimers in our spectra. The
209 oxidation product distributions in our experiments are in general term more diverse, i.e. we found
210 more compounds with smaller yields compared to Molteni et al. (2018). In our experiments the highest
211 20 compounds together explain 46 – 63 % of the total signal with the individual highest oxidation
212 products contributing only between 4.4 and 16%. These differences can be the result of different
213 experimental conditions and set up. In our study the residence time is almost double compared to
214 Molteni et al., leading to the formation of more oxidized compounds, especially more oxidized dimers,
215 which have been reported in this study. In addition we produce OH radicals [through irradiation at 254](#)
216 [nm](#) in the full length of the flow reactor enhancing the effects of secondary chemistry. Despite these
217 differences there is a general agreement on the conclusions for the NO_x free conditions with the
218 Molteni et al. study where one rapidly form HOM of very low volatility, that can initiate NPF.

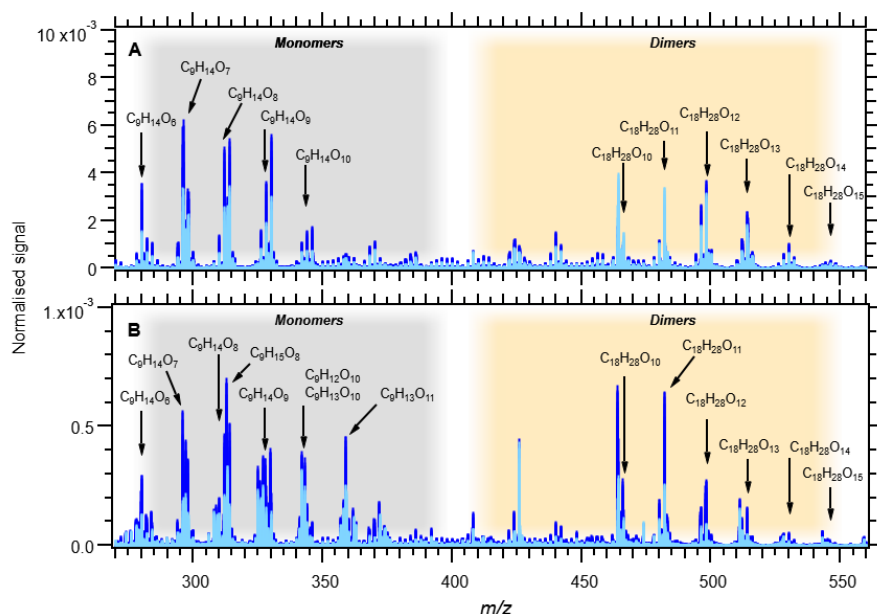
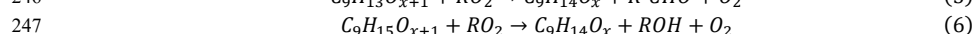
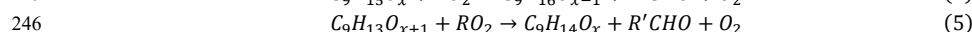
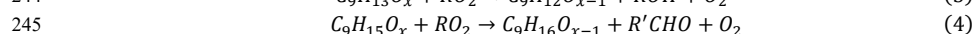
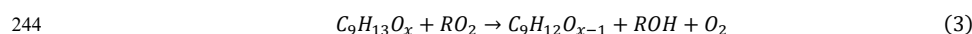


Figure 3: Mass spectra of all experiments without NO_x: 1, 2, 3, and 4. Panel A shows experiments 3 (light blue) and 4 (blue) with OH exposure of 2.87×10^{11} and 3.47×10^{11} molecules s cm⁻³ respectively. Panel B shows experiment 1 (light blue) and 2 (blue) with OH exposure of 3.47×10^{10} and 7.62×10^{10} molecules s cm⁻³ respectively. The signal at m/z 426 is associated with the used mass calibrant PFHA. Note the ten times lower Normalised Signal scale in B.

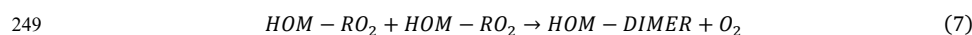
219 The amount of TMB reacted after 34 s in the experiments ranges from 30 ppb (almost all) in
 220 experiment 4 to 5 ppb in experiments 1 and NOx9 (comp. Table 1 and Figure S1). The signal
 221 intensities of the HOM monomers are increasing with increasing OH exposure. Dimer compounds also
 222 increase with increasing OH and reach their highest levels in exp 3, resulting in the highest ratio of
 223 dimer to monomer (see Figure 2). Faster conversion of TMB will result in higher initial RO₂ levels
 224 enabling faster RO₂ + RO₂ (self-) reaction. The concentration profile of RO₂ in exp 1 and 2 is lower
 225 and more evenly spread out over the length of Go:PAM (Figure S1) and the influence of the RO₂ +
 226 RO₂ reaction will be less in these experiments compared to exp 3 and 4. Enhanced OH exposure does
 227 not only affect the monomer/dimer ratio but also the total amount of compounds measured. Observed
 228 compounds were 10 times higher in the high OH exposure exp 3, 4, compared to exp 1, 2. This was
 229 also valid for the experiments with added NO_x (NOx1 and NOx3_H vs NOx3_L and NOx9). Under high
 230 OH exposure (exp 4) the major HOM monomer is C₉H₁₄O₇ with a contribution of 5.5 % to the total
 231 explained signal, followed by C₉H₁₆O₉ and C₉H₁₄O₈, contributing 4.6 and 4.5 % respectively.
 232 At the lowest OH exposure (exp 1) the major signals comprise the monomer C₉H₁₂O₁₀ and the dimers
 233 C₁₈H₂₆O₁₀ and C₁₈H₂₈O₁₁, contributing 4.4, 4.0 and 3.4 % to the total. These dimer compounds,
 234 C₁₈H₂₆O₁₀ and C₁₈H₂₈O₁₁, are the highest signals in exp 2 and 3. Two open shell species were found
 235 among the larger signals in exp 1 and 2 (see Figure 3): C₉H₁₅O₈ and C₉H₁₅O₇.

236 The number of H atoms is a characteristic for HOM monomers and dimers. An overview of
 237 different oxidation product generations is given in Table 2. We observe HOM monomers with 12-16 H

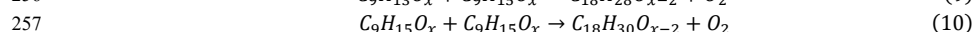
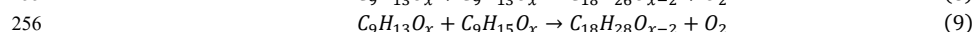
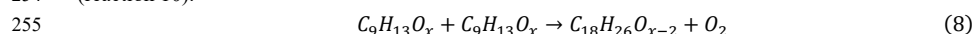
238 and all compounds with an even number of H are closed shell products. Compounds with an uneven
 239 number of H are open shell molecules (radicals). Following the proposed termination scheme by
 240 Mentel et al. (2015) compounds with 12 H can be identified as first generation monomers (terminated
 241 from $C_9H_{13}O_x$ radicals, reaction 3) and compounds with 16 H as second generation monomers
 242 (terminated from $C_9H_{15}O_x$ radicals, reaction 4). $C_9H_{14}O_x$ can be either first or second generation
 243 products and originate from either $C_9H_{13}O_x$ or $C_9H_{15}O_x$ (reactions 5 and 6).



248 The RO_2 radicals $C_9H_{13,15}O_x$ can form dimers likely via the reaction



250 Such reaction is possible between any HOM- RO_2 , first or second generation (and other C_9 peroxy
 251 radicals with sufficient high abundance). Two first generation HOM- RO_2 will result in $C_{18}H_{26}O_x$
 252 dimers (reaction 8) while one first and one second generation HOM- RO_2 produce a $C_{18}H_{28}O_x$ (reaction
 253 9) and dimerization of two second generation HOM- RO_2 will result in dimers of the formula $C_{18}H_{30}O_x$
 254 (reaction 10).



258 A closer examination of the contribution of different HOM generations in Table 2 shows that
 259 first generation monomers with 12 H are showing the highest contribution in experiments with low
 260 OH exposure (exp 1, 2) while monomers with 14 H gain importance with higher OH exposure. The
 261 second generation monomers with 16 H dominate in experiments with the highest OH exposure (exp
 262 3, 4). The dimer population with 28 H has a larger fraction of the total signal at higher OH exposures
 263 compared to dimers with 26 H. Dimer population with 30 H is generally lower than other dimers but
 264 has the highest fraction in exp 4. The overall dimer fraction of up to 43% in this study (Figure 2) is
 265 similar to the dimer fraction of 40% reported by Molteni et al. (2018). However, the relative
 266 contributions of monomer and dimer generations differ. We find higher contributions of H_{12}
 267 monomers (up to 11%) and a higher contribution of H_{28} dimer (up to 12%) under our experimental
 268 conditions. The contribution of H_{14} monomers and H_{26} dimers is significantly less compared to
 269 Molteni et al. (2018).

270 Increasing OH exposure promotes second OH attacks on oxidation products leading to the
 271 observed reduction of first generation products ($C_9H_{12}O_x$) as well as increase of second generation
 272 products ($C_9H_{14}O_x$ and $C_9H_{16}O_x$). The $C_9H_{14}O_x$ products have mainly characteristics of second
 273 generation products, as their contribution is enhanced in the experiments with higher OH exposures
 274 (Table S1), in which there is an enhanced possibility for secondary chemistry initiated by reaction of
 275 OH with the first generation products. The increased oxidation degree can also explain the formation
 276 of dimers ($C_{18}H_{28}O_x$) from first and second generation RO_2 ($C_9H_{13}O_x$ and $C_9H_{15}O_x$) at higher OH
 277 exposure and the increase in second generation dimers. Open shell species are observed as first
 278 generation RO_2 ($C_9H_{13}O_x$) and have a higher contribution lower at OH exposures. Second generation
 279 RO_2 ($C_9H_{15}O_x$) have the highest contribution in exp 3. At the highest OH exposures in exp 4, the
 280 contribution of $C_9H_{15}O_x$ radicals, one of the top ten contributors to the signal (Table S1), is reduced,

281 while the contribution of the second generation products ($C_9H_{14}O_x$ and $C_9H_{16}O_x$) and dimers
282 [increases/increased](#).

283

284

Table 2: Contribution of oxidation product families to the total signal between 270 – 560 m/z

Compound family	1	2	3	4	NO _x 9	NO _x 3 _L	NO _x 3 _H	NO _x 1
$C_9H_{12}O_x$	11.3	7.8	3.5	5.4	8.5	9.3	5.9	5.4
$C_9H_{13}O_x$	5.7	4.5	3.3	2.1	6.0	7.0	5.6	4.2
$C_9H_{14}O_x$	8.3	10.8	9.9	17.4	4.3	6.6	8.0	13.0
$C_9H_{15}O_x$	5.6	7.2	9.4	4.1	2.4	3.3	4.6	4.7
$C_9H_{16}O_x$	4.8	8.0	7.7	14.5	1.5	2.5	4.8	10.3
$C_{18}H_{26}O_x$	8.5	9.1	8.5	9.3	0.8	2.0	2.7	6.0
$C_{18}H_{28}O_x$	7.1	9.9	9.3	11.0	0.4	1.2	2.6	6.9
$C_{18}H_{30}O_x$	0.7	1.0	2.3	2.6	0.4	0.4	0.9	1.7
$C_9H_{13}NO_x$	6.2	4.7	0.6	0.6	26.8	17.1	10.1	4.8
$C_9H_{15}NO_x$	6.4	5.6	0.7	0.9	3.7	10.3	14.5	8.5
$C_9H_{14}N_2O_x$	2.1	1.7	1.0	1.1	18.7	11.8	7.5	1.9

285

286

287

288

289

290

In this study the contribution of $C_{18}H_{28}O_x$ shows that both first and second generation HOM- RO_2 were dimerising. The kinetics of dimer formation, if produced from RO_2 self-reaction, depends on the square of $[HOM-RO_2]$ and their relative importance will increase with the RO_2 concentration. Increased local RO_2 concentrations (in the first part of Go:PAM) would explain the increase of dimers with increasing OH exposure.

291

292

293

294

295

296

297

298

299

300

301

302

303

304

305

Substantial particle formation was observed in exp 4, under the highest OH exposure. Although the amount of reacted TMB in exp 3 and 4 is similar (26 and 30 ppb respectively), significant particle formation was not observed under the conditions of exp 3. The rate at which new particle formation (nucleation) occurs is related to the chemical composition and concentration of the nucleating species (McGraw and Zhang, 2008). After reaching the critical nucleus, particle growth becomes spontaneous in the presence of condensable vapour. Apparently, the local concentration of nucleating species or condensable vapour was not high enough in exp 3 to yield large numbers of particles, compared to exp 4. According to recent studies (Ehn et al., 2014; Trostl et al., 2016; Mohr et al., 2017; McFiggans et al., 2019) dimers play an important role in new particle formation. Mohr et al. (2017) found decreased levels of gas phase dimers in ambient air during NPF events, which is in line with our observations of lower dimer levels in the presence of particles in exp 4, compared to exp 3. A large enough concentration of low volatility dimers obviously helps forming critical nuclei that then grow by condensation. Note that the newly formed particles will provide an additional sink for dimers and thus reduce their presence as observable gas phase products at the end of the flow reactor.

306

Influence of NO_x

307

308

309

310

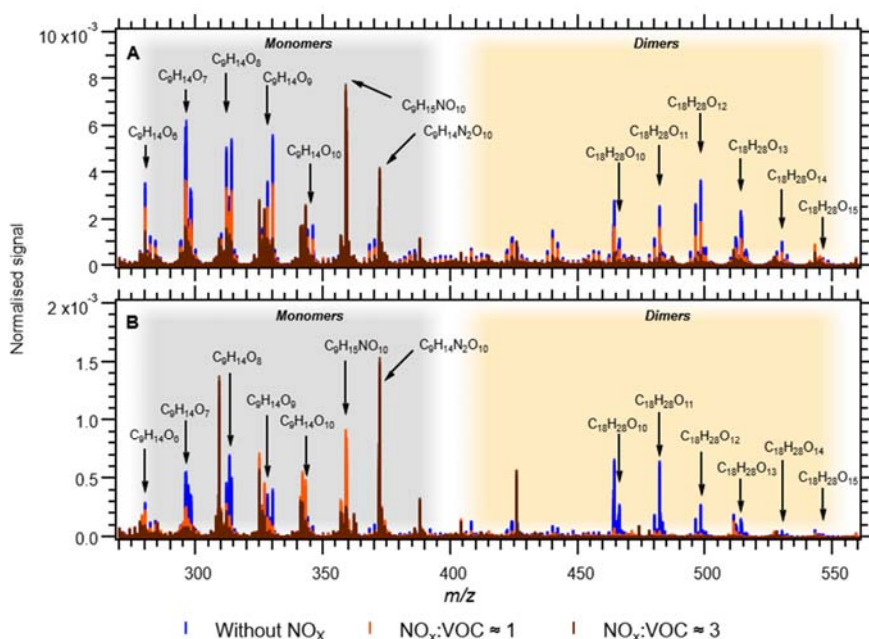
311

312

313

In the experiments NO_x1 , NO_x3_H , NO_x3_L and NO_x9 , the NO_x levels were increased (Table 1). As already has been described NO_x was introduced to the Go:PAM as NO. After the addition of ozone, the ozone concentration decreases from 100 ppb to ~80 ppb at the experiment with lower NO_x levels and to ~50 ppb at the experiment with higher NO_x levels, as it reacts with NO producing NO_2 . For both high and low NO_x conditions there is NO left after the initial reaction with ozone (see grey areas of Figure S3). The presence of NO_x gave nitrogen containing C_9 compounds with one or two N atoms and C_{18} compounds with only one N atom, in addition to HOM monomers and HOM dimers.

314 These compounds are expected to be nitrates or peroxy nitrates, as it is highly unlikely to form nitro-
 315 aromatic compounds from TMB (Sato et al., 2012). N-containing compounds were the dominating
 316 species in experiments with NO_x (see Figure 2), except for the experiment NO_x1 with the smallest
 317 amount of NO_x added and a high OH exposure (NO_x1). The amount of nitrated compounds increased
 318 with the amount of added NO_x at the expense of HOM monomers and HOM dimers as illustrated by
 319 the arrows in Figure 2. The effect of the added NO_x is attenuated at higher OH exposure. E.g., the
 320 nitrated monomers are reduced from 35.0 and 38.9% at low OH exposure down to 17.7 and 30.2% at
 321 high OH exposure. Under elevated NO_x conditions nitrated species were found among the 10
 322 compounds with the highest contribution to the respective total signal, (see the top-ten lists Table S1
 323 and Figure 4Figure-4).
 324



325
 326 **Figure 4: Comparison of mass spectra of HOM and nitrates.** Panel A shows experiment 4 (blue),
 327 NO_x1 (orange) and experiment NO_x3_H (brown). Panel B shows experiments 2 (blue), NO_x3_L
 328 (orange) and NO_x9 (brown).

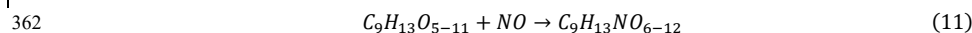
329 For the two experiments with low OH exposure where the nitrated species dominated, seven
 330 out of the top ten species were nitrated with the highest signal arising from the di-nitrated compound
 331 (C₉H₁₄N₂O₁₀). In these two experiments the top-ten compounds contributed the most to the observed
 332 signal (42.3 and 52.4%); most likely owing to the high fraction of nitrated species acting as radical
 333 chain termination products. Under highest NO_x conditions, the high OH exposure experiment
 334 (NO_x3_H) has six nitrated compounds in the top-ten list with the di-nitrated C₉H₁₄N₂O₁₀ on the second
 335 rank. In experiment NO_x1 only one nitrated species (C₉H₁₅NO₁₀) is found in the top-ten list despite the
 336 elevated NO_x conditions.

337 Dimer formation is drastically reduced in the presence of elevated NO_x. The NO_x effect on
 338 NPF was clear and high NO_x/ΔTMB suppresses NPF from TMB oxidation, a trend that was also

339 observed by Wildt et al. (2014) and Lehtipalo et al. (2018) for NPF from monoterpene oxidation.
 340 Whenever the products were dominated by ON (NOx3_L, NOx9 and NOx3_H) particle formation was not
 341 observed. Reduced particle formation was observed in NOx1 compared to exp 1 which had a higher
 342 contribution of HOM. Owing to the importance of dimers for NPF, as reported by Lehtipalo et al.
 343 (2018), we suggest that the reaction of RO₂ + NO resulting in ON is responsible for the observed
 344 reduced particle formation, because it competes with the dimer formation from RO₂ + RO₂. This
 345 reaction is also reducing the contribution of HOM monomers and dimers with increasing NO_x/ΔTMB
 346 and decreasing OH exposure from a total of 61% in exp NOx1 (OH exposure=9.1×10¹⁰ molecules s
 347 cm⁻³) to 27.5% in NOx9 (OH exposure=6.3×10⁹ molecules s cm⁻³). The reaction RO₂ + NO reduce the
 348 amount of HOM monomers and dimers in competing with autoxidation and termination by RO₂+RO₂
 349 or RO₂+HO₂. The yield of ON from NO+RO₂ might be high-significant (e.g. up to 0.3) based on the
 350 measurable increase of ON and the decrease of NO_x in the system (Figure S3).

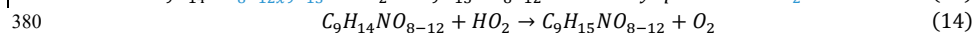
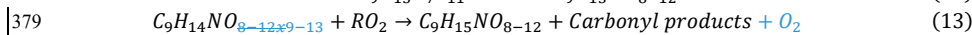
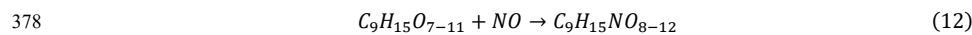
351 The contribution of HOM monomer generations follows the general trend observed in
 352 experiments without NO_x. The first generation HOM have higher contribution at low OH exposures in
 353 NOx3_L and NOx9 and the contribution of second generation HOM is higher the higher the OH
 354 exposure is. Similarly, the contribution of C₉H₁₄O_x is increasing with increasing OH exposure.
 355 Analogously to the families of HOM, different families of nitrates can be defined. Table 2 gives an
 356 overview of the nitrate families and how they contribute to the total signal in the experiments. At
 357 lowest OH exposures we find the highest contributions of first generation nitrates (C₉H₁₃NO_x) as well
 358 as di-nitrates (C₉H₁₄N₂O_x). The contribution of second generation nitrates (C₉H₁₅NO_x) is increasing
 359 with increasing OH exposure and is highest in NOx3_H.

360 For the formation of observed first generation nitrates C₉H₁₃NO₆₋₁₂ (C₉H₁₃NO_x in [Table](#)
 361 [2Table-2](#)) we propose the reaction of a first generation (HOM-)RO₂ with NO following the pathway:



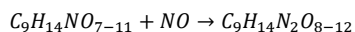
363 The precursor C₉H₁₃O₅ is formed after one autoxidation step and its termination reaction with NO
 364 results in C₉H₁₃NO₆ which has only minor contribution. C₉H₁₃NO_{7&8}, with higher contribution in exp
 365 NOx3_L and NOx9 can be formed from the radicals C₉H₁₃O₆ and C₉H₁₃O₇ respectively. The even
 366 oxygen number in C₉H₁₃O₆ indicates that the compound should have undergone a transformation to
 367 RO (via reaction with RO₂ or NO) and subsequent H-shift and further O₂ addition (Vereecken and
 368 Peeters, 2010; Mentel et al., 2015). A proposed detailed reaction mechanism is depicted in the Figure
 369 5.

370 Second generation nitrates (C₉H₁₅NO₈₋₁₂) can be formed after an additional OH attack (and
 371 introduction of an additional H) on a first generation (HOM) monomer, which explains the increase of
 372 these compounds with increasing OH exposure. The termination of the RO₂ radical chain with NO
 373 (reaction 12) will then lead to the formation of the second generation nitrate. The formation of RO₂
 374 precursor species with 7-8 O numbers, i.e. C₉H₁₅O_{7,8} likely stem from compounds terminated earlier in
 375 the radical chain process (C₉H₁₄O_{4,5}), which do not fall in the typical HOM class (O:C ≥ 6:9). The
 376 reaction of a first generation nitrate with OH, followed by autoxidation could also possibly produce
 377 C₉H₁₅NO₈₋₁₂ by terminating via peroxy (reaction 13) or hydroperoxy pathway (reaction 14).



381 For the formation of the most abundant di-nitrates of the formula C₉H₁₄N₂O₈₋₁₂ (reaction 15), OH has
 382 to attack a nitrated compound C₉H₁₃NO₆₋₁₀ and the RO₂ radical chain has to be terminated with NO
 383 (Figure 5).

384

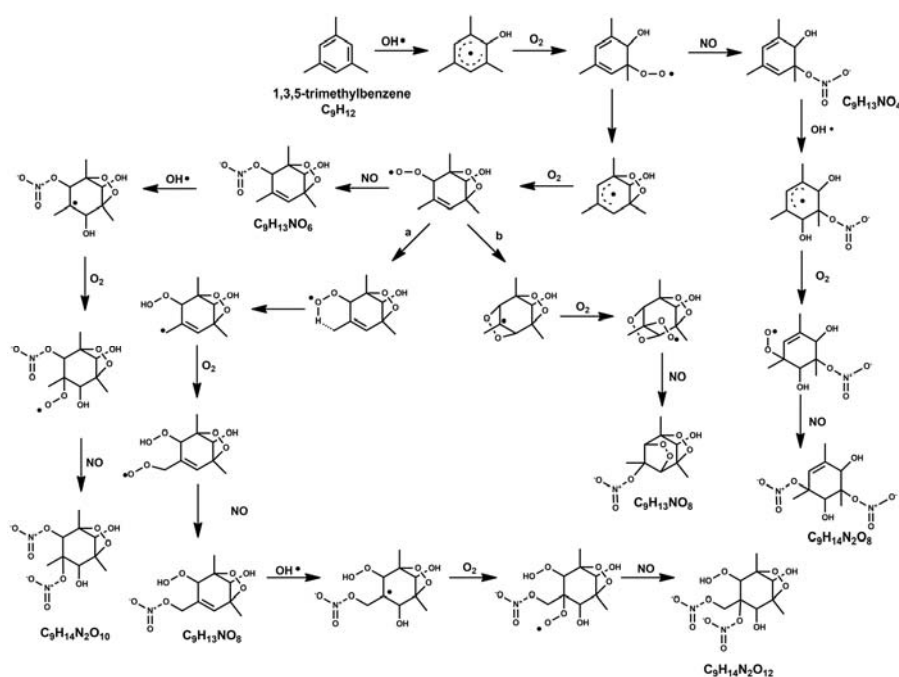


(15)

385 The precursor species $C_9H_{14}NO_7$ would be in this case formed from the OH attack on the smallest
386 possible nitrate $C_9H_{13}NO_4$ (formed after one autoxidation step and NO termination).

387 It should be noted that the formation of peroxy nitrates via the reaction $RO_2 + NO_2 \rightarrow RO_2NO_2$ with
388 alkyl and acyl- RO_2 (PAN-like) cannot be ruled out as a potential formation mechanisms of nitrates.

389 The volatility of the produced ON seems to be too high (compared to dimers) to initiate NPF at the
390 present concentrations as seen from the reduction in particle formation potential from exp 4 (HOM
391 dominated, particle formation) to NOx1 (reduction in HOM and increase in ON, reduced particle
392 formation) and NOx3H (ON dominated, no particle formation).



393

394 **Figure 5: The proposed radical reaction mechanism for the formation of some of the mono- and**
395 **di-nitrates from TMB mentioned in this study. Two separate mechanisms were suggested for the**
396 **species with the formula $C_9H_{13}NO_8$, which formation pathways are based on (a) (Wang et al.,**
397 **2017) and (b) (Molteni et al., 2018).**

398 Figure 2B shows the results for the evolution of HOM monomer, HOM Dimers and organic
399 nitrates (ON) as calculated using the kinetic model described in detailed in SI. The model used has a
400 very simplified scheme for TMB oxidation and subsequent RO_2 chemistry. We implemented a few
401 rate coefficients suggested in the literature in order to demonstrate how those compare with our
402 experimental results. Rate coefficients for RO_2 termination reactions from MCM in combination with
403 rate coefficients of dimer formation by Berndt et al. (2018) (case 1 and 2 in SI Table S2) led to an
404 overestimation of dimer compounds. Better representation of the observations were achieved by
405 applying a) the rate coefficients proposed by (Zhao et al., 2018) for dimer formation (2.0×10^{-12}
406 $cm^3 molecules^{-1} s^{-1}$) and $1.0 \times 10^{-12} cm^3 molecules^{-1} s^{-1}$ for termination and RO formation with branching

407 ratios of 0.4 and 0.6, respectively; b) the rate coefficient ($1.0 \times 10^{-11} \text{ cm}^3 \text{ molecules}^{-1} \text{ s}^{-1}$) from Berndt et
408 al. (2018) for $\text{HOMRO}_2 + \text{NO}$ with a branching ratio of 0.3 for ON formation (reaction 56 in Table
409 S2).

410 In Figure 2B, the calculated HOM dimer contribution are the sum of medium (produced from
411 $\text{HOM-RO}_2 + \text{RO}_2$), and highly oxidised dimers (produced from $\text{HOM-RO}_2 + \text{HOM-RO}_2$) while the ON
412 includes both organic nitrates (produced from $\text{HOM-RO}_2 + \text{NO}$) and peroxy nitrates (produced from
413 $\text{HOM-RO}_2 + \text{NO}_2$). The increased production of monomers calculated for exp 1 and 2 is in agreement
414 with experimental results, where we observed a slightly larger contribution from monomers compared
415 to dimers. Calculated concentrations for dimers are similar in exp 3 and higher in exp 4, compared to
416 monomers. Secondary chemistry (reaction of OH with the products and possible formation of a second
417 generation of HOM or nitrates) was not taken into consideration in the model. For the experiment with
418 NO_x (Figure 2B, right panels) the modeled product distribution follows the general trend of monomer,
419 dimer and nitrate that we observe in the exp NOx3_L and NOx9 with a general higher nitrate production
420 compared to monomers and dimers. For the NO_x experiments with high initial ozone, the model can
421 reproduce the higher HOM monomer and dimer levels in NOx1 but slightly overestimates the
422 contribution of dimers. Particle formation was observed in NOx1 which might explain the
423 overestimation owing to missing condensation sink in the model. Modelling NOx3_H gives an
424 overestimation of monomers and dimers.

425 In NOx3_H modelled dimers start forming after ~ 15 sec. Almost all NO is converted to ON or NO_2 at
426 this point and the reaction $\text{HOM-RO}_2 + \text{NO}$ does not produce additional ON and the modelled levels of
427 ON reach a plateau while contribution of HOM dimers can increase. For exp NOx1 and NOx3_H the
428 model is in better agreement with the measurements if only the HOM - dimer formation (from $\text{HOM-RO}_2 + \text{HOM-RO}_2$)
429 is taken into account, i.e. highly oxidized dimers excluding medium oxidized dimer
430 (from $\text{HOM-RO}_2 + \text{RO}_2$). Generally, the simplified model was able to support our analysis of the
431 TMB chemistry as described above. Furthermore, it gave some support to the recently suggested
432 mechanisms included in case 3 (e.g. (Zhao et al., 2018))
433

434 4 Atmospheric implication and Conclusion

435 We have measured the formation of HOM monomers and dimers from OH initiated oxidation
436 of TMB. The experiments with highest OH exposures lead to particle formation when NO_x was not
437 added. With increasing OH exposure and increased likelihood of a second OH attack, we observe a
438 higher contribution from second generation oxidation products and dimers in general. The latter is
439 attributed to the increased RO_2 concentrations from the increased/fast TMB consumption by OH. The
440 observed products in this study match what would be expected as termination products from
441 previously proposed reaction mechanisms for HOM formation.

442 The addition of NO_x to simulate urban condition leads to the formation of ON in addition to
443 HOM and a reduction in particle formation potential. We observe that the formation of ON is
444 increasing with increasing $\text{NO}_x/\Delta\text{TMB}$, mostly at the expense of dimers. The presence of ONs, formed
445 at the expense of dimers, can explain the decreased tendency for particle formation. We therefore
446 suggest that the reaction $\text{HOM-RO}_2 + \text{NO}$ competes with HOM-RO_2 self-reaction yielding primarily a
447 reduction in dimer formation, which is responsible for the reduction in particle formation. The
448 experimental designed using the Go:PAM with concentrations of HO_x (and RO_x) higher than ambient
449 would attenuate the influence of added NO_x . This will further emphasis the implication of our findings
450 and most likely the NO_x effect would be even more important in the urban atmosphere.

Formatted: Subscript

Formatted: Subscript

Formatted: Subscript

Formatted: Subscript

451 According to studies by (Molteni et al., 2018) and (Wang et al., 2017) HOM formation from
452 AVOCs was observed and consequently AVOC-HOM were suggested as potential contributors to
453 observed NPF in urban atmospheres. In our study, under NO_x free conditions, we found several of
454 previous identified HOM even if we did not fully agree with the identity and relative importance of all
455 HOM. However, the oxidation in polluted environments will happen under elevated NO_x levels and, as
456 has been shown here this can lead to formation of ON instead of HOM and subsequently a reduction in
457 NPF potential. We conclude that for interpretation of NPF from aromatics in urban areas care should
458 be taken and the OH exposure, NO_x levels and RO₂ concentrations need to be considered in details
459 since they will largely determine if the HOM-RO₂+NO can compete with reactions yielding HOM,
460 and especially HOM dimers.

461
462

463 *Data availability:* The data set is available upon request by contacting Mattias Hallquist
464 (hallq@chem.gu.se).

465 *Competing Interests:* The authors declare that they have no conflict of interest.

466 *Author contribution:* J.H., E.T. T.M. and M.H. designed the experiments. J.H and E.T performed the
467 experiments and data analysis. E.T. performed the modelling. C.M.S. designed the chemical
468 mechanisms. E.T., J.H. and M.H. wrote the paper. All authors commented on the paper and were
469 involved in the scientific interpretation and discussion.

470 *Acknowledgements:* The research presented is a contribution to the Swedish strategic research area
471 Modelling the Regional and Global Earth system, MERGE. This work was supported by the Swedish
472 Research Council (grant numbers 2014-05332; 2013-06917) and Formas (grant number 2015-1537).

473

474 5. References:

475

- 476 Atkinson, R., Baulch, D. L., Cox, R. A., Hampson, R. F., Kerr, J. A., and Troe, J.: Evaluated Kinetic and Photochemical Data
477 for Atmospheric Chemistry Supplement-Iv - Iupac Subcommittee on Gas Kinetic Data Evaluation for Atmospheric
478 Chemistry, *J Phys Chem Ref Data*, 21, 1125-1568, Doi 10.1063/1.555918, 1992.
- 479 Berndt, T., Richters, S., Jokinen, T., Hyttinen, N., Kurten, T., Otkjaer, R. V., Kjaergaard, H. G., Stratmann, F., Herrmann, H.,
480 Sipila, M., Kulmala, M., and Ehn, M.: Hydroxyl radical-induced formation of highly oxidized organic compounds, *Nat*
481 *Commun*, 7, 13677, 10.1038/ncomms13677, 2016.
- 482 Bianchi, F., Trostl, J., Junninen, H., Frege, C., Henne, S., Hoyle, C. R., Molteni, U., Herrmann, E., Adamov, A., Bukowiecki,
483 N., Chen, X., Duplissy, J., Gysel, M., Hutterli, M., Kangasluoma, J., Kontkanen, J., Kurten, A., Manninen, H. E.,
484 Munch, S., Perakyla, O., Petaja, T., Rondo, L., Williamson, C., Weingartner, E., Curtius, J., Worsnop, D. R., Kulmala,
485 M., Dommen, J., and Baltensperger, U.: New particle formation in the free troposphere: A question of chemistry and
486 timing, *Science*, 352, 1109-1112, 10.1126/science.aad5456, 2016.
- 487 Bianchi, F., Garmash, O., He, X., Yan, C., Iyer, S., Rosendahl, I., Xu, Z., Rissanen, M. P., Riva, M., Taipale, R., Sarnela, N.,
488 Petäjä, T., Worsnop, D. R., Kulmala, M., Ehn, M., and Junninen, H.: The role of highly oxygenated molecules (HOMs)
489 in determining the composition of ambient ions in the boreal forest, *Atmos Chem Phys*, 17, 13819-13831, 10.5194/acp-
490 17-13819-2017, 2017.
- 491 Bianchi, F., Kurten, T., Riva, M., Mohr, C., Rissanen, M. P., Roldin, P., Berndt, T., Crouse, J. D., Wennberg, P. O., Mentel,
492 T. F., Wildt, J., Junninen, H., Jokinen, T., Kulmala, M., Worsnop, D. R., Thornton, J. A., Donahue, N., Kjaergaard, H.
493 G., and Ehn, M.: Highly Oxygenated Organic Molecules (HOM) from Gas-Phase Autoxidation Involving Peroxy
494 Radicals: A Key Contributor to Atmospheric Aerosol, *Chem Rev*, 119, 3472-3509, 10.1021/acs.chemrev.8b00395,
495 2019.
- 496 Chan, C. K., and Yao, X.: Air pollution in mega cities in China, *Atmos Environ*, 42, 1-42, 10.1016/j.atmosenv.2007.09.003,
497 2008.
- 498 Crouse, J. D., Nielsen, L. B., Jorgensen, S., Kjaergaard, H. G., and Wennberg, P. O.: Autoxidation of Organic Compounds
499 in the Atmosphere, *J Phys Chem Lett*, 4, 3513-3520, 10.1021/jz4019207, 2013.
- 500 Donahue, N. M., Kroll, J. H., Pandis, S. N., and Robinson, A. L.: A two-dimensional volatility basis set – Part 2: Diagnostics
501 of organic-aerosol evolution, *Atmos. Chem. Phys.*, 12, 615-634, 10.5194/acp-12-615-2012, 2012.
- 502 Ehn, M., Kleist, E., Junninen, H., Petäjä, T., Lönn, G., Schobesberger, S., Dal Maso, M., Trimbom, A., Kulmala, M.,
503 Worsnop, D. R., Wahner, A., Wildt, J., and Mentel, T. F.: Gas phase formation of extremely oxidized pinene reaction
504 products in chamber and ambient air, *Atmos Chem Phys*, 12, 5113-5127, 10.5194/acp-12-5113-2012, 2012.

505 Ehn, M., Thornton, J. A., Kleist, E., Sipila, M., Junninen, H., Pullinen, I., Springer, M., Rubach, F., Tillmann, R., Lee, B.,
506 Lopez-Hilfiker, F., Andres, S., Acir, I.-H., Rissanen, M., Jokinen, T., Schobesberger, S., Kangasluoma, J., Kontkanen,
507 J., Nieminen, T., Kurten, T., Nielsen, L. B., Jorgensen, S., Kjaergaard, H. G., Canagaratna, M., Maso, M. D., Berndt,
508 T., Petaja, T., Wahner, A., Kerminen, V.-M., Kulmala, M., Worsnop, D. R., Wildt, J., and Mentel, T. F.: A large source
509 of low-volatility secondary organic aerosol, *Nature*, 506, 476-479, 10.1038/nature13032, 2014.

510 Eisele, F. L., and Tanner, D. J.: Measurement of the gas phase concentration of H₂SO₄ and methane sulfonic acid and
511 estimates of H₂SO₄ production and loss in the atmosphere, *Journal of Geophysical Research: Atmospheres*, 98, 9001-
512 9010, 10.1029/93jd00031, 1993.

513 Finlayson-Pitts, B. a. P., J.: *Chemistry of the Upper and Lower Atmosphere*, 1999.

514 Gentner, D. R., Jathar, S. H., Gordon, T. D., Bahreini, R., Day, D. A., El Haddad, I., Hayes, P. L., Pieber, S. M., Platt, S. M.,
515 de Gouw, J., Goldstein, A. H., Harley, R. A., Jimenez, J. L., Prevot, A. S. H., and Robinson, A. L.: Review of Urban
516 Secondary Organic Aerosol Formation from Gasoline and Diesel Motor Vehicle Emissions, *Environmental science &*
517 *technology*, 51, 1074-1093, 10.1021/acs.est.6b04509, 2017.

518 Guo, S., Hu, M., Zamora, M. L., Peng, J., Shang, D., Zheng, J., Du, Z., Wu, Z., Shao, M., Zeng, L., Molina, M. J., and
519 Zhang, R.: Elucidating severe urban haze formation in China, *Proc Natl Acad Sci U S A*, 111, 17373-17378,
520 10.1073/pnas.1419604111, 2014.

521 Hallquist, M., Wenger, J. C., Baltensperger, U., Rudich, Y., Simpson, D., Claeys, M., Dommen, J., Donahue, N. M., George,
522 C., Goldstein, A. H., Hamilton, J. F., Herrmann, H., Hoffmann, T., Iinuma, Y., Jang, M., Jenkin, M. E., Jimenez, J. L.,
523 Kiendler-Scharr, A., Maenhaut, W., McFiggans, G., Mentel, T. F., Monod, A., Prevot, A. S. H., Seinfeld, J. H., Surratt,
524 J. D., Szmigielski, R., and Wildt, J.: The formation, properties and impact of secondary organic aerosol: current and
525 emerging issues, *Atmos. Chem. Phys.*, 9, 5155-5236, 2009.

526 Hallquist, M., Munthe, J., Hu, M., Wang, T., Chan, C. K., Gao, J., Boman, J., Guo, S., Hallquist, A. M., Mellqvist, J.,
527 Moldanova, J., Pathak, R. K., Pettersson, J. B. C., Pleijel, H., Simpson, D., and Thynell, M.: Photochemical smog in
528 China: scientific challenges and implications for air-quality policies, *National Science Review*, 3, 401-403,
529 10.1093/nsr/nww080, 2016.

530 Hu, M., Guo, S., Peng, J.-f., and Wu, Z.-j.: Insight into characteristics and sources of PM_{2.5} in the Beijing-Tianjin-Hebei
531 region, China, *National Science Review*, 2, 257-258, 10.1093/nsr/nwv003, 2015.

532 Huang, M., Lin, Y., Huang, X., Liu, X., Guo, X., Hu, C., Zhao, W., Gu, X., Fang, L., and Zhang, W.: Experimental study of
533 particulate products for aging of 1,3,5-trimethylbenzene secondary organic aerosol, *Atmos Pollut Res*, 6, 209-219,
534 10.5094/apr.2015.025, 2015.

535 Intergovernmental Panel on Climate, C.: *Climate Change 2013 - The Physical Science Basis*, Cambridge University Press,
536 Cambridge, United Kingdom and New York, NY, USA, 1535 pp., 2014.

537 Jokinen, T., Sipila, M., Junninen, H., Ehn, M., Lonn, G., Hakala, J., Petaja, T., Mauldin, R. L., Kulmala, M., and Worsnop,
538 D. R.: Atmospheric sulphuric acid and neutral cluster measurements using CI-API-TOF, *Atmos. Chem. Phys.*, 12,
539 4117-4125, 10.5194/acp-12-4117-2012, 2012.

540 Jokinen, T., Sipila, M., Richters, S., Kerminen, V. M., Paasonen, P., Stratmann, F., Worsnop, D., Kulmala, M., Ehn, M.,
541 Herrmann, H., and Berndt, T.: Rapid autoxidation forms highly oxidized RO₂ radicals in the atmosphere, *Angewandte*
542 *Chemie (International ed. in English)*, 53, 14596-14600, 10.1002/anie.201408566, 2014.

543 Jokinen, T., Berndt, T., Makkonen, R., Kerminen, V. M., Junninen, H., Paasonen, P., Stratmann, F., Herrmann, H., Guenther,
544 A. B., Worsnop, D. R., Kulmala, M., Ehn, M., and Sipila, M.: Production of extremely low volatile organic compounds
545 from biogenic emissions: Measured yields and atmospheric implications, *Proc. Natl. Acad. Sci. U.S.A.*, 112, 7123-7128,
546 10.1073/pnas.1423977112, 2015.

547 Junninen, H., Ehn, M., Petaja, T., Luosujarvi, L., Kotiaho, T., Kostianen, R., Rohner, U., Gonin, M., Fuhrer, K., Kulmala,
548 M., and Worsnop, D. R.: A high-resolution mass spectrometer to measure atmospheric ion composition, *Atmospheric*
549 *Measurement Techniques*, 3, 1039-1053, 10.5194/amt-3-1039-2010, 2010.

550 Kang, E., Root, M. J., Toohey, D. W., and Brune, W. H.: Introducing the concept of Potential Aerosol Mass (PAM), *Atmos.*
551 *Chem. Phys.*, 7, 5727-5744, DOI 10.5194/acp-7-5727-2007, 2007.

552 Kirkby, J., Duplissy, J., Sengupta, K., Frege, C., Gordon, H., Williamson, C., Heinritzi, M., Simon, M., Yan, C., Almeida, J.,
553 Trostl, J., Nieminen, T., Ortega, I. K., Wagner, R., Adamov, A., Amorim, A., Bernhammer, A. K., Bianchi, F.,
554 Breitenlechner, M., Brilke, S., Chen, X., Craven, J., Dias, A., Ehrhart, S., Flagan, R. C., Franchin, A., Fuchs, C., Guida,
555 R., Hakala, J., Hoyle, C. R., Jokinen, T., Junninen, H., Kangasluoma, J., Kim, J., Krapf, M., Kurten, A., Laaksonen, A.,
556 Lehtipalo, K., Makhmutov, V., Mathot, S., Molteni, U., Onnela, A., Perakyla, O., Piel, F., Petaja, T., Praplan, A. P.,
557 Pringle, K., Rap, A., Richards, N. A., Riipinen, I., Rissanen, M. P., Rondo, L., Sarnela, N., Schobesberger, S., Scott, C.
558 E., Seinfeld, J. H., Sipila, M., Steiner, G., Stozhkov, Y., Stratmann, F., Tome, A., Virtanen, A., Vogel, A. L., Wagner,
559 A. C., Wagner, P. E., Weingartner, E., Wimmer, D., Winkler, P. M., Ye, P., Zhang, X., Hansel, A., Dommen, J.,
560 Donahue, N. M., Worsnop, D. R., Baltensperger, U., Kulmala, M., Carslaw, K. S., and Curtius, J.: Ion-induced
561 nucleation of pure biogenic particles, *Nature*, 533, 521-526, 10.1038/nature17953, 2016.

562 Kristensen, K., Watne, A. K., Hammes, J., Lutz, A., Petäjä, T., Hallquist, M., Bilde, M., and Glasius, M.: High-Molecular
563 Weight Dimer Esters Are Major Products in Aerosols from α -Pinene Ozonolysis and the Boreal Forest, *Environmental*
564 *Science & Technology Letters*, 3, 280-285, 10.1021/acs.estlett.6b00152, 2016.

565 Kurtén, T., Tiisanen, K., Roldin, P., Rissanen, M., Luy, J.-N., Boy, M., Ehn, M., and Donahue, N.: α -Pinene Autoxidation
566 Products May Not Have Extremely Low Saturation Vapor Pressures Despite High O:C Ratios, *The Journal of Physical*
567 *Chemistry A*, 120, 2569-2582, 10.1021/acs.jpca.6b02196, 2016.

568 Lee, B. H., Mohr, C., Lopez-Hilfiker, F. D., Lutz, A., Hallquist, M., Lee, L., Romer, P., Cohen, R. C., Iyer, S., Kurtén, T.,
569 Hu, W., Day, D. A., Campuzano-Jost, P., Jimenez, J. L., Xu, L., Ng, N. L., Guo, H., Weber, R. J., Wild, R. J., Brown,
570 S. S., Koss, A., de Gouw, J., Olson, K., Goldstein, A. H., Seco, R., Kim, S., McAvey, K., Shepson, P. B., Starn, T.,
571 Baumann, K., Edgerton, E. S., Liu, J., Shilling, J. E., Miller, D. O., Brune, W., Schobesberger, S., D'Ambro, E. L., and

572 Thornton, J. A.: Highly functionalized organic nitrates in the southeast United States: Contribution to secondary
573 organic aerosol and reactive nitrogen budgets, *Proceedings of the National Academy of Sciences*, 113, 1516-1521,
574 10.1073/pnas.1508108113, 2016.

575 McFiggans, G., Mentel, T. F., Wildt, J., Pullinen, I., Kang, S., Kleist, E., Schmitt, S., Springer, M., Tillmann, R., Wu, C.,
576 Zhao, D., Hallquist, M., Faxon, C., Le Breton, M., Hallquist, A. M., Simpson, D., Bergstrom, R., Jenkin, M. E., Ehn,
577 M., Thornton, J. A., Alfarra, M. R., Bannan, T. J., Percival, C. J., Priestley, M., Topping, D., and Kiendler-Scharr, A.:
578 Secondary organic aerosol reduced by mixture of atmospheric vapours, *Nature*, 565, 587-593, 10.1038/s41586-018-
579 0871-y, 2019.

580 McGraw, R., and Zhang, R.: Multivariate analysis of homogeneous nucleation rate measurements. Nucleation in the p-toluic
581 acid/sulfuric acid/water system, *The Journal of chemical physics*, 128, 064508, 10.1063/1.2830030, 2008.

582 Mentel, T. F., Springer, M., Ehn, M., Kleist, E., Pullinen, I., Kurtén, T., Rissanen, M., Wahner, A., and Wildt, J.: Formation
583 of highly oxidized multifunctional compounds: autoxidation of peroxy radicals formed in the ozonolysis of alkenes –
584 deduced from structure–product relationships, *Atmos. Chem. Phys.*, 15, 6745-6765, 10.5194/acp-15-6745-2015, 2015.

585 Mohr, C., Lopez-Hilfiker, F. D., Yli-Juuti, T., Heitto, A., Lutz, A., Hallquist, M., D'Ambro, E. L., Rissanen, M. P., Hao, L.
586 Q., Schobesberger, S., Kulmala, M., Mauldin, R. L., Makkonen, U., Sipilä, M., Petaja, T., and Thornton, J. A.: Ambient
587 observations of dimers from terpene oxidation in the gas phase: Implications for new particle formation and growth,
588 *Geophys Res Lett*, 44, 2958-2966, 10.1002/2017gl072718, 2017.

589 Molteni, U., Bianchi, F., Klein, F., El Haddad, I., Frege, C., Rossi, M. J., Dommen, J., and Baltensperger, U.: Formation of
590 highly oxygenated organic molecules from aromatic compounds, *Atmospheric Chemistry and Physics*, 18, 1909-1921,
591 10.5194/acp-18-1909-2018, 2018.

592 Paulsen, D., Dommen, J., Kalberer, M., Prevot, A. S., Richter, R., Sax, M., Steinbacher, M., Weingartner, E., and
593 Baltensperger, U.: Secondary organic aerosol formation by irradiation of 1,3,5-trimethylbenzene-NO_x-H₂O in a new
594 reaction chamber for atmospheric chemistry and physics, *Environ Sci Technol*, 39, 2668-2678, 10.1021/es0489137,
595 2005.

596 Rodigast, M., Mutzel, A., and Hermann, H.: A quantification method for heat-decomposable methylglyoxal oligomers and
597 its application on 1,3,5-trimethylbenzene SOA, *Atmos. Chem. Phys.*, 17, 3929-3943, 10.5194/acp-17-3929-2017, 2017.

598 Sato, K., Takami, A., Kato, Y., Seta, T., Fujitani, Y., Hikida, T., Shimono, A., and Imamura, T.: AMS and LC/MS analyses
599 of SOA from the photooxidation of benzene and 1,3,5-trimethylbenzene in the presence of NO_x: effects of chemical
600 structure on SOA aging, *Atmos. Chem. Phys.*, 12, 4667-4682, 10.5194/acp-12-4667-2012, 2012.

601 Shrivastava, M., Cappa, C. D., Fan, J. W., Goldstein, A. H., Guenther, A. B., Jimenez, J. L., Kuang, C., Laskin, A., Martin, S.
602 T., Ng, N. L., Petaja, T., Pierce, J. R., Rasch, P. J., Roldin, P., Seinfeld, J. H., Shilling, J., Smith, J. N., Thornton, J. A.,
603 Volkamer, R., Wang, J., Worsnop, D. R., Zaveri, R. A., Zelenyuk, A., and Zhang, Q.: Recent advances in
604 understanding secondary organic aerosol: Implications for global climate forcing, *Rev. Geophys.*, 55, 509-559,
605 10.1002/2016rg000540, 2017.

606 Trostl, J., Chuang, W. K., Gordon, H., Heinritzi, M., Yan, C., Molteni, U., Ahlm, L., Frege, C., Bianchi, F., Wagner, R.,
607 Simon, M., Lehtipalo, K., Williamson, C., Craven, J. S., Duplissy, J., Adamov, A., Almeida, J., Bernhammer, A. K.,
608 Breitenlechner, M., Brilke, S., Dias, A., Ehrhart, S., Flagan, R. C., Franchin, A., Fuchs, C., Guida, R., Gysel, M.,
609 Hansel, A., Hoyle, C. R., Jokinen, T., Junninen, H., Kangasluoma, J., Keskinen, H., Kim, J., Krapf, M., Kurten, A.,
610 Laaksonen, A., Lawler, M., Leiminger, M., Mathot, S., Mohler, O., Nieminen, T., Onnela, A., Petaja, T., Piel, F. M.,
611 Miettinen, P., Rissanen, M. P., Rondo, L., Sarnela, N., Schobesberger, S., Sengupta, K., Sipilä, M., Smith, J. N.,
612 Steiner, G., Tome, A., Virtanen, A., Wagner, A. C., Weingartner, E., Wimmer, D., Winkler, P. M., Ye, P. L., Carslaw,
613 K. S., Curtius, J., Dommen, J., Kirkby, J., Kulmala, M., Riipinen, I., Worsnop, D. R., Donahue, N. M., and
614 Baltensperger, U.: The role of low-volatility organic compounds in initial particle growth in the atmosphere, *Nature*,
615 533, 527+, 10.1038/nature18271, 2016.

616 Wang, S., Wu, R., Berndt, T., Ehn, M., and Wang, L.: Formation of Highly Oxidized Radicals and Multifunctional Products
617 from the Atmospheric Oxidation of Alkylbenzenes, *Environ Sci Technol*, 51, 8442-8449, 10.1021/acs.est.7b02374,
618 2017.

619 Watne, Å. K., Psychoudaki, M., Ljungström, E., Le Breton, M., Hallquist, M., Jerksjö, M., Fallgren, H., Jutterström, S., and
620 Hallquist, Å. M.: Fresh and Oxidized Emissions from In-Use Transit Buses Running on Diesel, Biodiesel, and CNG,
621 *Environmental science & technology*, 52, 7720-7728, 10.1021/acs.est.8b01394, 2018.

622 Vereecken, L., and Peeters, J.: A structure–activity relationship for the rate coefficient of H-migration in substituted alkoxy
623 radicals, 10.1039/C0CP00387E, 2010.

624 WHO: Ambient air pollution: A global assessment of exposure and burden of disease, 2016.

625 Wyche, K. P., Monks, P. S., Ellis, A. M., Cordell, R. L., Parker, A. E., Whyte, C., Metzger, A., Dommen, J., Duplissy, J.,
626 Prevot, A. S. H., Baltensperger, U., Rickard, A. R., and Wulfert, F.: Gas phase precursors to anthropogenic secondary
627 organic aerosol: detailed observations of 1,3,5-trimethylbenzene photooxidation, *Atmos. Chem. Phys.*, 9, 635-665, DOI
628 10.5194/acp-9-635-2009, 2009.

629 Yan, C., Nie, W., Aijala, M., Rissanen, M. P., Canagaratna, M. R., Massoli, P., Junninen, H., Jokinen, T., Sarnela, N., Hame,
630 S. A. K., Schobesberger, S., Canonaco, F., Yao, L., Prevot, A. S. H., Petaja, T., Kulmala, M., Sipilä, M., Worsnop, D.
631 R., and Ehn, M.: Source characterization of highly oxidized multifunctional compounds in a boreal forest environment
632 using positive matrix factorization, *Atmos. Chem. Phys.*, 16, 12715-12731, 10.5194/acp-16-12715-2016, 2016.

633 Zhao, Y., Thornton, J. A., and Pye, H. O. T.: Quantitative constraints on autoxidation and dimer formation from direct
634 probing of monoterpene-derived peroxy radical chemistry, *Proc. Natl. Acad. Sci. U. S. A.*, 115, 12142-12147,
635 10.1073/pnas.1812147115, 2018.